

Remote control of ion channels and neurons through magnetic-field heating of nanoparticles

Heng Huang¹, Savas Delikanli¹, Hao Zeng¹, Denise M. Ferkey² and Arnd Pralle^{1*}

Recently, optical stimulation^{1–3} has begun to unravel the neuronal processing that controls certain animal behaviours^{4,5}. However, optical approaches are limited by the inability of visible light to penetrate deep into tissues. Here, we show an approach based on radio-frequency magnetic-field heating of nanoparticles to remotely activate temperature-sensitive cation channels in cells. Superparamagnetic ferrite nanoparticles were targeted to specific proteins on the plasma membrane of cells expressing TRPV1, and heated by a radio-frequency magnetic field. Using fluorophores as molecular thermometers, we show that the induced temperature increase is highly localized. Thermal activation of the channels triggers action potentials in cultured neurons without observable toxic effects. This approach can be adapted to stimulate other cell types and, moreover, may be used to remotely manipulate other cellular machinery for novel therapeutics.

Analysing complex networks in animals using electrical or optical methods is challenging, because electrical fields are strongly attenuated by tissues. Magnetic fields are promising for truly remote stimulation because they interact weakly with biological molecules and can penetrate deep into the body. However, their weak interaction with biological molecules means that the magnetic fields need to be translated into a different stimulus such as mechanical force or torque^{6,7} or aggregation of particles⁸ to act on their target. Because force or torque generation requires the use of large micrometre-sized beads, it is unsuitable for many *in vivo* applications. Although small (30 nm) nanoparticles have been used to induce the aggregation of cell receptors⁸, whole-body applications remain challenging because a locally focused and strong spatial field gradient is required.

Here, we present an approach using local heating of superparamagnetic nanoparticles to convert a radio-frequency (RF) magnetic signal into cell stimulation. Manganese ferrite (MnFe₂O₄) nanoparticles ($d = 6$ nm) were targeted to cells expressing the temperature-sensitive ion channel TRPV1, and heated using a RF magnetic field. The local temperature increase opened the TRPV1 channels and caused an influx of calcium ions (schematic in Fig. 1a). The activation temperature of the TRPV1 protein is 42 °C (refs 9,10), which is close enough to normal body temperature to permit quick stimulation while allowing the channels to be normally closed. In addition, TRPV1 has been heterologously expressed in *Drosophila* neurons and stimulated with capsaicin to successfully evoke behavioural responses¹¹. Our approach can activate cells uniformly across a large volume, making it feasible for *in vivo* whole-body applications. We further show that this approach can be adapted to remotely trigger behavioural responses in *Caenorhabditis elegans* worms.

An aqueous dispersion of MnFe₂O₄ nanoparticles (20 mg ml⁻¹, $d = 6$ nm)^{12–14} conjugated with streptavidin¹⁵ and subjected to a RF

magnetic field (40 MHz, 8.4 G) heats up at an initial rate of 0.62 °C s⁻¹ (Supplementary Fig. S1). This field strength satisfies the Food and Drug Administration requirements for RF fields applied during magnetic resonance imaging (MRI; Supplementary Fig. S1). This bulk solution heating was measured by a thermocouple, but for biological applications the local temperature is more important and has proven challenging to measure.

Here, we show how the temperature dependence of the fluorescence intensity of fluorophores can be used as a molecular-scale temperature probe. Figure 1b displays the temperature dependence of the fluorescence intensity and lifetime of the DyLight549 fluorophore bound to streptavidin (see Supplementary Information for the temperature dependence of fluorescence intensity for other fluorophores; Fig. S3)^{16,17}. The detailed photophysics of the temperature dependence, which may be attributed to destabilized excited states and increased rate of non-radiative relaxation¹⁸, remains to be investigated (Heng *et al.*, manuscript in preparation).

Using chemically targeted fluorophores as a thermometer, we recorded the temperature distribution around nanoparticles in aqueous dispersions and in cells. The surface temperature of the nanoparticles was measured using the emission intensity from DyLight549 conjugated to the streptavidin coating the nanoparticles, and the bulk solution temperature was measured using yellow fluorescent protein (YFP) dispersed in the solution (Fig. 1c, inset). In a dilute dispersion of nanoparticles (~10 nM), a heating rate of 0.31 °C s⁻¹ was measured at the nanoparticle surface in response to the magnetic field; but there was no heating of the bulk solution. This concentration of 10 nM corresponds to an average nanoparticle separation of 1 μm, far below the 20-μm minimal concentration required for bulk solution heating (see Supplementary Information for modelling of the heat dissipation; Fig. S2). We conclude that the immediate surface of an isolated nanoparticle heats significantly above the ambient temperature, but the temperature around each nanoparticle decays too rapidly to cause appreciable bulk heating.

To effectively heat the TRPV1 channels to stimulate specific cells *in vivo*, a high local density of nanoparticles would be required to cause significant regional heating, that is, along the membrane surface. We achieve this *in vitro* by targeting the streptavidin-conjugated nanoparticles to cells of interest, which have been genetically made to express the engineered membrane protein marker AP-CFP-TM (Fig. 2d; see Methods). This protein marker contains a transmembrane domain (TM) of the platelet-derived growth factor, an extracellular fluorescent protein (CFP) and a biotin acceptor peptide (AP)^{19,20} that is enzymatically biotinylated to bind the streptavidin-conjugated nanoparticle.

To study the temperature profile, we used the temperature dependence of the fluorescence intensity of DyLight549 (conjugated to the streptavidin-coated nanoparticles on the cell membrane) and

¹Department of Physics, University at Buffalo, the State University of New York, Buffalo, New York 14260, USA, ²Department of Biological Sciences, University at Buffalo, the State University of New York, Buffalo, New York 14260, USA. *e-mail: apralle@buffalo.edu

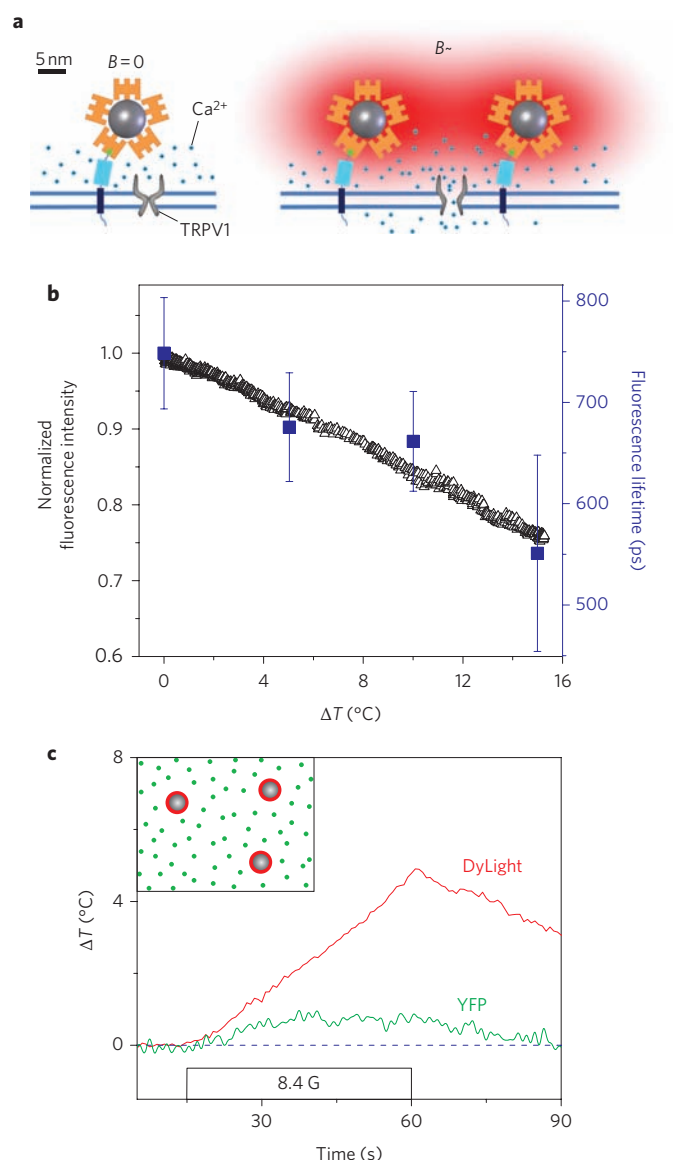


Figure 1 | Principles of ion channel stimulation using nanoparticle heating and local temperature sensing. **a**, Schematic, drawn to scale, showing local heating of streptavidin-DyLight549 (orange)-coated superparamagnetic nanoparticles (grey) in a RF magnetic field ($B \sim$) and heat (red)-induced opening of TRPV1. The AP-CFP-TM protein binds the nanoparticles through the biotinylated AP domain (green box), which is anchored to the membrane by the TM (blue box) and CFP (cyan box) domains. **b**, Temperature dependence of the fluorescence intensity and lifetime of streptavidin-DyLight549 ($\Delta F/F = -1.5\% \text{ } ^\circ\text{C}^{-1}$, measured in an externally heated nanoparticle dispersion). **c**, Applying a RF magnetic field to a nanoparticle dispersion increased the nanoparticle surface temperature (red trace, change in temperature measured by DyLight549 fluorescence) while only moderately changing the solution temperature (green trace, change in temperature measured by YFP fluorescence). Inset shows a schematic of the nanoparticle dispersion (green dots represent YFP; red rings indicate the streptavidin-DyLight549 coating around the nanoparticles (grey)).

Golgi-targeted green fluorescent protein (GFP) (co-expressed within the cell) as nanoscale thermometers (Fig. 2e). As soon as a RF magnetic field was applied, the cell surface DyLight549 fluorescence intensity decreased, indicating heating of more than $15 \text{ } ^\circ\text{C}$ within 15 s, while the GFP fluorescence intensity in the Golgi remained virtually unchanged. This clearly demonstrates that the heating is limited to the immediate vicinity of the plasma

membrane. In further experiments that tested the remote activation of the TRPV1 channels, we maintained the plasma membrane temperature at less than $43 \text{ } ^\circ\text{C}$ to avoid damaging the membrane.

In recent years, magnetic hyperthermia has been extensively investigated in the field of cancer therapy^{21,22}. A major challenge has been to achieve a sufficiently high concentration of nanoparticles for bulk solution heating. Our approach, in which a high density of nanoparticles is confined to a small volume, for example, in the plasma membrane, results in efficient local heating while requiring significantly fewer nanoparticles to be delivered to the organism. We therefore anticipate that our approach could be adapted to therapeutic applications.

To study whether nanoparticle-generated local heat is sufficient to trigger the opening of TRPV1 channels, we measured the intracellular calcium concentration using the genetically encoded, Förster resonance energy transfer (FRET)-based calcium sensor, Troponin extra large (TN-XL)²³. Human embryonic kidney cells (HEK 293) expressing TRPV1 and TN-XL were specifically labelled with streptavidin-coated nanoparticles via the biotinylated AP-CFP-TM membrane protein. Within 15 s of applying the RF magnetic field (40 MHz, 8.4 G) the cytosolic calcium concentration increased from about 100 nM to $1.6 \text{ } \mu\text{M}$ (according to the TN-XL calcium titration curve²³, Fig. 3a). The increase was found to be caused by calcium influx through thermally activated TRPV1 channels, because cells with nanoparticles but without TRPV1 channels, and cells with TRPV1 channels but without nanoparticles, did not show any calcium influx upon application of the same RF magnetic field (Supplementary Table S1). For comparison, calcium influx into HEK 293 cells was evoked by capsaicin (Fig. 3a). These data show that RF magnetic-field-induced nanoparticle heating is sufficient to trigger the opening of TRPV1 channels within seconds.

The magnetic-field-induced calcium influx results in a neuronal depolarization that is sufficient to elicit an action potential, which is necessary for the control of neuronal function. We measured changes in the membrane potential of hippocampal neurons that expressed TRPV1 and were labelled with nanoparticles, using the voltage-sensitive dye ANNINE6²⁴. Immediately after applying the RF magnetic field, the ANNINE6 fluorescence intensity decreased as the membrane temperature rose (Fig. 3b). When the membrane temperature reached $\sim 40 \text{ } ^\circ\text{C}$, the voltage-sensitive dye registered several small membrane voltage spikes followed by an action-potential-type depolarization (Fig. 3b, inset). We conclude that the remote activation of cationic TRPV1 channels by means of nanoparticle heating is sufficient to induce action potentials in neurons without causing cellular damage. This is a promising approach for remotely stimulating neurons, because the magnetic field can penetrate deep into the body.

As an example for the remote triggering of a behavioural response in live animals, we show the initiation of a thermal avoidance reaction in *C. elegans*. When *C. elegans* encounter a heated probe, they reflex and initiate backward locomotion²⁵. Because it is not known which neurons are involved in this noxious thermosensation, we targeted all sensory neurons in the amphid region with nanoparticles rather than labelling one specific cell. The nanoparticles were coated with polyethylene glycol (PEG)-phospholipid²⁶, which enriched them in the mucus layer, protecting the amphid region (Fig. 4d)²⁷. The crawling of single worms was tracked while applying a RF magnetic field. Within 5 s of applying this stimulus, the worms halted their forward locomotion, and soon afterwards reversed (34 of 40 worms stopped, and of these, 27 subsequently reversed). (For a typical response of a worm see Supplementary Movie S1, for simultaneous stimulation of a group of worms see Movie S2 and for all *C. elegans* data see Table S2.) Worms subjected to the same field but not labelled with nanoparticles did not halt their forward locomotion (Supplementary Movie S3).

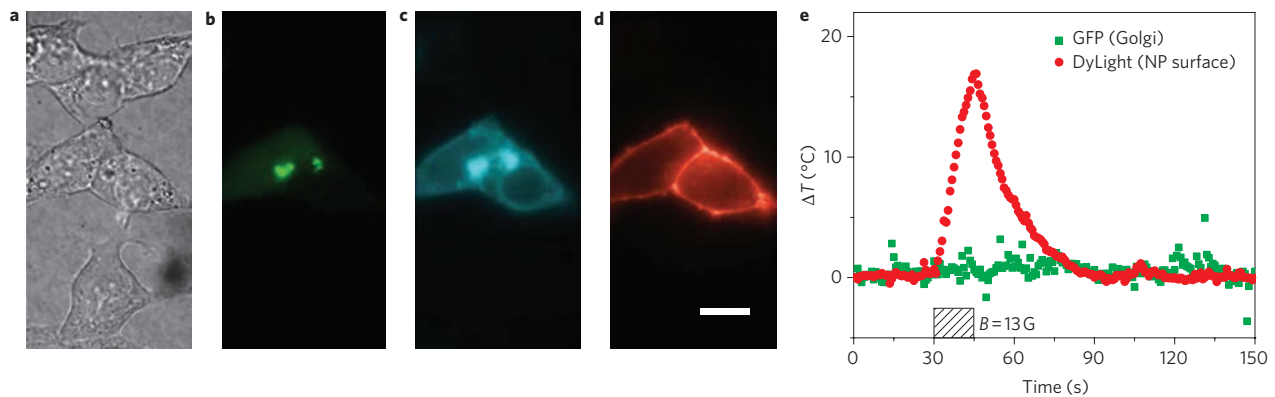


Figure 2 | Genetic targeting of nanoparticles to specific cells and localized membrane heating. **a-d**, Microscopy images showing a group of HEK 293 cells, two of which are expressing Golgi-targeted GFP and the biotinylated membrane protein AP-CFP-TM (ref. 19). Differential interference contrast (DIC) image displaying all cells (**a**), green fluorescence image indicating the Golgi localized GFP (**b**), cyan fluorescence marking the membrane protein AP-CFP-TM (**c**), red fluorescence of the DyLight549 (**d**) on the nanoparticles, which are exclusively localized on the plasma membrane of the AP-CFP-TM expressing cells. Scale bar, 20 μm . **e**, During application of the RF magnetic field ($t = 30\text{--}45$ s as indicated by the hatched box), the local temperature increased at the plasma membrane (red, measured by the change in DyLight549 fluorescence intensity), yet remained constant at the Golgi apparatus (green, measured by fluorescence intensity of Golgi-targeted GFP).

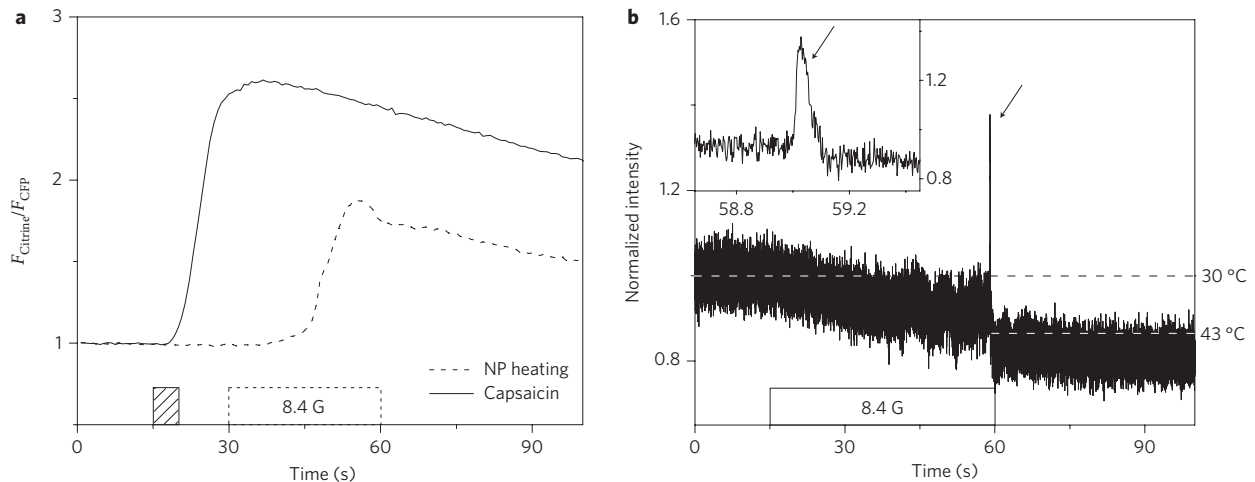


Figure 3 | Opening of TRPV1 channels and activation of action potentials. **a**, TRPV1 opening and calcium influx in HEK 293 cells as a result of capsaicin stimulation (solid line) or nanoparticle (NP) heating (dashed line). The calcium influx was measured as the Citrine/CFP fluorescence intensity ratio of the calcium indicator TN-XL. Magnetic field stimulation of nanoparticle-coated cells (30 s, 40 MHz, 8.4 G, white box) evoked a similar calcium influx as stimulation with 2 μM capsaicin (5 s, hatched box). **b**, Action potentials were elicited in nanoparticle-coated, cultured hippocampal neurons, which heterologously expressed TRPV1. The membrane potential was recorded using the voltage-sensitive dye ANNINE6. During application of the RF magnetic field, the intensity of the ANNINE6 fluorescence decreased as the membrane temperature increased from 30 to 43 $^{\circ}\text{C}$, at which point firing of an action potential was observed. Inset: magnified view of the action potential (arrow).

The similar response of all the worms within the magnetic field demonstrates a major advantage of this method, in that it does not require the stimulating energy field to be focused onto one cell or animal, which would be challenging when stimulating a large group of animals or cells within one organism simultaneously.

To show that this response was indeed due to local heating of the amphid, and to measure the threshold temperature for the behavioural response, we incubated the worms with fluorescein-labelled PEG-coated nanoparticles. As soon as the magnetic field was applied, the fluorescein intensity decreased, indicating heating of the amphid area (Fig. 4a, Supplementary Movie S4). Five seconds later the fluorescein indicated a local temperature of 34 $^{\circ}\text{C}$, and the worm retracted despite being partially anaesthetized by being mounted on a thin agarose pad containing 9 mM NaN_3 (ref. 28; Fig. 4b). This temperature

threshold is consistent with the previously reported noxious temperature²⁵, and suggests that our approach can be adapted to whole-animal studies.

In summary, we have established remote control of ion channels in cells using RF magnetic-field heating of nanoparticles. We have demonstrated the potential of this approach to study neuronal signalling and adapted it to trigger behavioural responses in worms. In addition, we have used fluorescence as a nanometre-scale thermometer, showing that the heat is generated locally to the membrane without cytoplasmic heating. Future work will focus on genetically targeting streptavidin-coated nanoparticles to selected neurons in *C. elegans*, transferring the method to studies in the mammalian brain, and optimizing the local concentration of heating for apoptosis in hyperthermia cancer therapy.

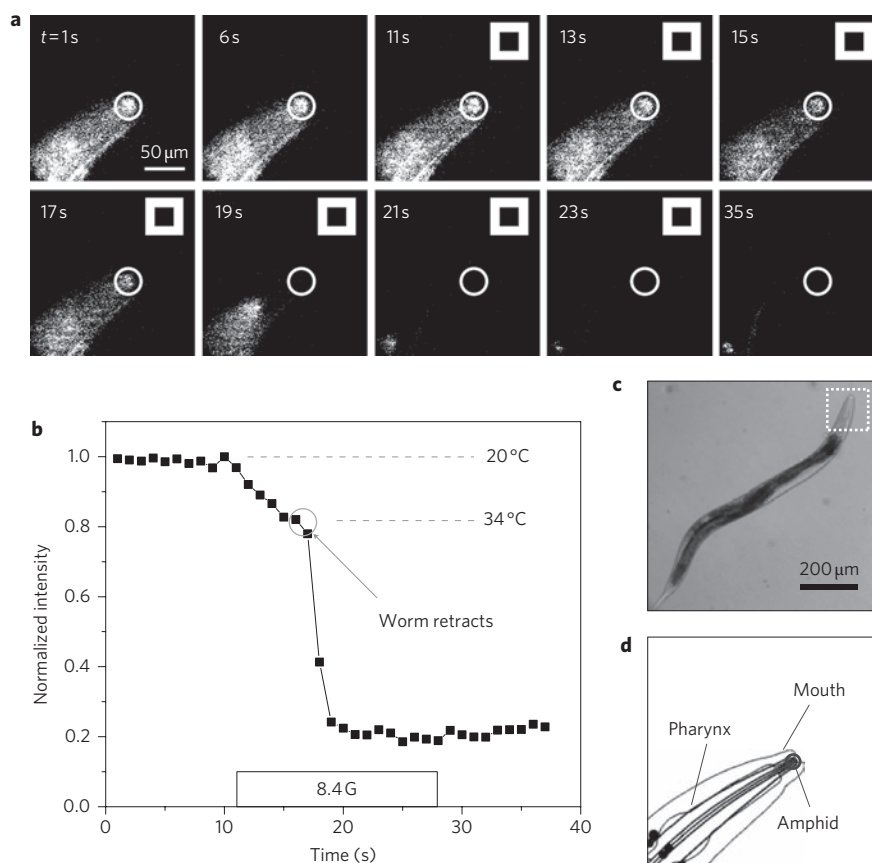


Figure 4 | Remote stimulation of thermal avoidance response in *C. elegans*. **a**, Fluorescence image sequence of the head region of a *C. elegans* worm that has been labelled with fluorescein-PEG-coated nanoparticles and anaesthetized with sodium azide (Supplementary Movie S4). During application of the RF magnetic field between 11 and 28 s (square boxes in movie frames), the fluorescein fluorescence intensity decreased. This decrease corresponds to a temperature increase from 20 to 34 °C ($t = 17$ s), at which point the worm retracted. **b**, Plot of the time course of the fluorescence intensity and temperature for the amphid region. **c**, Bright-field image of the *C. elegans* worm, indicating the head region shown in the image sequence in **a**. **d**, Schematic highlighting the basic structures of the head region, where the dendrites of multiple sensory neurons reach the external environment (via the amphid pore).

Methods

Cell and *C. elegans* culture and imaging. HEK 293 cells, rat hippocampal neurons and *C. elegans* were maintained, transfected and imaged according to standard procedures (for details see Supplementary Information).

Nanoparticle synthesis and functionalization. Manganese ferrite (MnFe_2O_4) nanoparticles (6 nm) were synthesized according to published procedures¹². See Supplementary Information and references^{12,13} for details of synthesis. They were made water-dispersible by surface ligand exchange and coated with 2,3-dimercaptosuccinic acid (DMSA) following modified procedures by Jun and Lee¹⁴. MnFe_2O_4 nanoparticle dispersion (200 μl) in hexane was washed with methanol to remove excess surfactant oleylamine. The precipitants were redissolved in hexane and added dropwise into a DMSA solution (9 mg ml^{-1}) in methanol. The precipitated nanoparticles were washed with acetone, dried, and dissolved in 200 μl of 2.5% NH_4OH solution. The pH value of the nanoparticle aqueous solution was adjusted to 8.0 by flowing nitrogen gas above the solution to accelerate reduction of NH_4^+ to NH_3 .

For further stabilization, and to provide a means for specific targeting, the nanoparticles were conjugated with streptavidin¹⁵. The nanoparticles were conjugated with streptavidin-DyLight-549 (Pierce) using succinimidyl-4-[*N*-maleimidomethyl]-cyclohexane-1-carboxylate (SMCC, Pierce) as cross-linker. The final hydrodynamic radius of the nanoparticles was expected to be 6 to 8 nm.

Nanoparticle targeting to cell membrane and amphid of *C. elegans*. The cells of interest were genetically labelled by expressing the engineered membrane marker protein AP-CFP-TM, which contains a transmembrane domain (TM) of the platelet-derived growth factor, an extracellular cyan fluorescent protein (CFP) and a biotin acceptor peptide (AP)^{19,20}. The biotin acceptor peptide was enzymatically biotinylated by the co-expressed BirA protein, forming specific binding sites for the streptavidin-conjugated nanoparticles.

For experiments with *C. elegans*, the nanoparticles were PEG-phospholipid coated following procedures similar to those of Grancharov and colleagues²⁶, in

which 60 μl of MnFe_2O_4 nanoparticle solution in hexane was washed with methanol to remove the surfactant oleylamine. The precipitants were dissolved in 650 μl of chloroform, and 60 μl of DSPE-methoxy PEG (2000) (10 mg ml^{-1}), 60 μl of maleimide-PEG (2000) (10 mg ml^{-1}) and 30 μl of DSPE-PEG (2000)-carboxy fluorescein (0.5 mg ml^{-1}) (all from Avanti Polar Lipids) were then added to the chloroform solution and mixed for 1 h in the dark. After evaporating the chloroform, the phospholipid-coated nanoparticles were dissolved in 600 μl of distilled water and incubated at 80 °C for 12 h before removing excess PEG-phospholipids.

RF magnetic-field and bulk solution heating. A 40 MHz sinusoidal signal was provided by a signal generator (Marconi Instruments), amplified by a 100 W amplifier (Amplifier Research), and applied to a 25-turn solenoid coil with a diameter of 7 mm. The magnetic field strength was adjusted between 0.67 and 1 kA m^{-1} (8.4 to 13 G). The coil was insulated with a 500- μm coating and positioned directly above the sample using a micromanipulator.

When subjected to a RF magnetic field (40 MHz, 8.4 G), the temperature in an aqueous dispersion of the DMSA-coated nanoparticles (20 mg ml^{-1}) increased at an initial rate of 0.62 °C s^{-1} , as measured with a thermocouple. This heating corresponds to a specific absorption rate (SAR) of 2.51 J $\text{g}^{-1} \text{s}^{-1}$ (Supplementary Fig. S1).

Local heat quantification. Local temperature changes were measured by recording the changes in fluorescence intensity of fluorophores (DyLight549, YFP or ANNINE6), subtracting the bleach rate, and converting it into a temperature change based on the measured temperature dependence of the fluorescence intensity. The $\Delta F(T)/F(T_0)$ of these fluorophores are -1.5% for DyLight549, -1.3% for YFP, -0.81% for ANNINE6 and -1.2% for fluorescein (Supplementary Fig. S3).

Received 7 March 2010; accepted 19 May 2010;
published online 27 June 2010

References

1. Zemelman, B. V., Lee, G. A., Ng, M. & Miesenbock, G. Selective photostimulation of genetically charged neurons. *Neuron* **33**, 15–22 (2002).
2. Boyden, E. S., Zhang, F., Bamberg, E., Nagel, G. & Deisseroth, K. Millisecond-timescale, genetically targeted optical control of neural activity. *Nature Neurosci.* **8**, 1263–1268 (2005).
3. Banghart, M., Borges, K., Isacoff, E., Trauner, D. & Kramer, R. H. Light-activated ion channels for remote control of neuronal firing. *Nature Neurosci.* **7**, 1381–1386 (2004).
4. Tsai, H. C. *et al.* Phasic firing in dopaminergic neurons is sufficient for behavioral conditioning. *Science* **324**, 1080–1084 (2009).
5. Gradinaru, V., Mogri, M., Thompson, K. R., Henderson, J. M. & Deisseroth, K. Optical deconstruction of parkinsonian neural circuitry. *Science* **324**, 354–359 (2009).
6. Wang, N., Butler, J. P. & Ingber, D. E. Mechanotransduction across the cell surface and through the cytoskeleton. *Science* **260**, 1124–1127 (1993).
7. Hughes, S., McBain, S., Dobson, J. & El Haj, A. J. Selective activation of mechanosensitive ion channels using magnetic particles. *J. R. Soc. Interface* **5**, 855–863 (2008).
8. Mannix, R. J. *et al.* Nanomagnetic actuation of receptor-mediated signal transduction. *Nature Nanotech.* **3**, 36–40 (2008).
9. Caterina, M. J. *et al.* The capsaicin receptor: a heat-activated ion channel in the pain pathway. *Nature* **389**, 816–824 (1997).
10. Tominaga, M. *et al.* The cloned capsaicin receptor integrates multiple pain-producing stimuli. *Neuron* **21**, 531–543 (1998).
11. Lima, S. Q. & Miesenbock, G. Remote control of behavior through genetically targeted photostimulation of neurons. *Cell* **121**, 141–152 (2005).
12. Zeng, H., Rice, P. M., Wang, S. X. & Sun, S. Shape-controlled synthesis and shape-induced texture of MnFe₂O₄ nanoparticles. *J. Am. Chem. Soc.* **126**, 11458–11459 (2004).
13. Sun, S. *et al.* Monodisperse MFe₂O₄ (M = Fe, Co, Mn) nanoparticles. *J. Am. Chem. Soc.* **126**, 273–279 (2004).
14. Jun, Y.-W. *et al.* Nanoscale size effect of magnetic nanocrystals and their utilization for cancer diagnosis via magnetic resonance imaging. *J. Am. Chem. Soc.* **127**, 5732–5733 (2005).
15. Lee, J.-H. *et al.* Artificially engineered magnetic nanoparticles for ultra-sensitive molecular imaging. *Nature Med.* **13**, 95–99 (2007).
16. Duhr, S., Arduini, S. & Braun, D. Thermophoresis of DNA determined by microfluidic fluorescence. *Eur. Phys. J. E* **15**, 277–286 (2004).
17. Kalab, P., Pralle, A., Isacoff, E. Y., Heald, R. & Weis, K. Analysis of a RanGTP-regulated gradient in mitotic somatic cells. *Nature* **440**, 697–701 (2006).
18. Karstens, T. & Kobs, K. Rhodamine B and Rhodamine 101 as reference substances for fluorescence quantum yield measurements. *J. Phys. Chem.* **84**, 1871–1872 (1980).
19. Howarth, M., Takao, K., Hayashi, Y. & Ting, A. Y. Targeting quantum dots to surface proteins in living cells with biotin ligase. *Proc. Natl Acad. Sci. USA* **102**, 7583–7588 (2005).
20. Howarth, M. & Ting, A. Y. Imaging proteins in live mammalian cells with biotin ligase and monovalent streptavidin. *Nature Protoc.* **3**, 534–545 (2008).
21. Hilger, I. *et al.* Evaluation of temperature increase with different amounts of magnetite in liver tissue samples. *Invest. Radiol.* **32**, 705–712 (1997).
22. Hergt, R. *et al.* Maghemite nanoparticles with very high AC-losses for application in RF-magnetic hyperthermia. *J. Magn. Magn. Mater.* **270**, 345–357 (2004).
23. Mank, M. *et al.* A FRET-based calcium biosensor with fast signal kinetics and high fluorescence change. *Biophys. J.* **90**, 1790–1796 (2006).
24. Hübener, G., Lambacher, A. & Fromherz, P. Anellated hemicyanine dyes with large symmetrical solvatochromism of absorption and fluorescence. *J. Phys. Chem. B* **107**, 7896–7902 (2003).
25. Wittenburg, N. & Baumeister, R. Thermal avoidance in *Caenorhabditis elegans*: an approach to the study of nociception. *Proc. Natl Acad. Sci. USA* **96**, 10477–10482 (1999).
26. Grancharov, S. G. *et al.* Bio-functionalization of monodisperse magnetic nanoparticles and their use as biomolecular labels in a magnetic tunnel junction based sensor. *J. Phys. Chem. B* **109**, 13030–13035 (2005).
27. Wang, Y. Y. *et al.* Addressing the PEG mucoadhesivity paradox to engineer nanoparticles that ‘slip’ through the human mucus barrier. *Angew. Chem. Int. Ed.* **47**, 9726–9729 (2008).
28. Wood, W. B. *The Nematode Caenorhabditis elegans* (Cold Spring Harbor Laboratory, 1988).

Acknowledgements

The authors thank F. Qin for the TRPV1 plasmid and initial assistance, A. Ting for the biotin acceptor peptide-cyan fluorescent protein-transmembrane (AP-CFP-TM) and BirA constructs, and O. Griesbeck for the TN-XL plasmid. J. Pazik is acknowledged for technical assistance, and Y. Hsu, V. Rana, M.J. Ezak and M. Zugravu for valuable discussions.

Author contributions

A.P. designed the study. H.H. carried out nanoparticle coating and cellular measurements. S.D. and H.Z. were responsible for nanoparticle synthesis and characterization, and D.M.F. for the *C. elegans* experiments. A.P. and H.H. wrote the manuscript. All authors discussed the results and commented on the manuscript. The work was supported by NSF DMR-0547036, UB IRDF, RF and INSIE.

Additional information

The authors declare no competing financial interests. Supplementary information accompanies this paper at www.nature.com/naturenanotechnology. Reprints and permission information is available online at <http://npg.nature.com/reprintsandpermissions/>. Correspondence and requests for materials should be addressed to A.P.